LAPPEENRANTA UNIVERSITY OF TECHNOLOGY

LUT School of Energy Systems

LUT Mechanical Engineering

Pekka Marttinen

REAL-TIME MONITORING OF LASER SCRIBING PROCESS UTILIZING HIGH-SPEED CAMERA

Examiners: Prof. Antti Salminen

D. Sc. Hamid Roozbahani

ABSTRARCT

Lappeenranta University of Technology
LUT School of Energy Systems
LUT Mechanical Engineering

Pekka Marttinen

REAL-TIME MONITORING OF LASER SCRIBING PROCESS UTILIZING HIGH-SPEED CAMERA

Currently, laser scribing is growing material processing method in the industry. Benefits of laser scribing technology are studied for example for improving an efficiency of solar cells. Due high-quality requirement of the fast scribing process, it is important to monitor the process in real time for detecting possible defects during the process. However, there is a lack of studies of laser scribing real time monitoring. Commonly used monitoring methods developed for other laser processes such a laser welding, are sufficient slow and existed applications cannot be implemented in fast laser scribing monitoring. The aim of this thesis is to find a method for laser scribing monitoring with a high-speed camera and evaluate reliability and performance of the developed monitoring system with experiments. The laser used in experiments is an IPG ytterbium pulsed fiber laser with 20 W maximum average power and Scan head optics used in the laser is Scanlab's Hurryscan 14 II with an f100 tele-centric lens. The camera was connected to laser scanner using camera adapter to follow the laser process. A powerful fully programmable industrial computer was chosen for executing image processing and analysis. Algorithms for defect analysis, which are based on particle analysis, were developed using LabVIEW system design software. The performance of the algorithms was analyzed by analyzing a non-moving image from the scribing line with resolution 960x20 pixel. As a result, the maximum analysis speed was 560 frames per second. Reliability of the algorithm was evaluated by imaging scribing path with a variable number of defects 2000 mm/s when the laser was turned off and image analysis speed was 430 frames per second. The experiment was successful and as a result, the algorithms detected all defects from the scribing path. The final monitoring experiment was performed during a laser process. However, it was challenging to get active laser illumination work with the laser scanner due physical dimensions of the laser lens and the scanner. For reliable error detection, the illumination system is needed to be replaced.

TIIVISTELMÄ

Pekka Marttinen

REAALIAIKAINEN LASERKAIVERRUSPROSESSIN MONITOROINTI SUURNOPEUSKAMERALLA

Tällä hetkellä laser kaiverrus on kasvava materiaalityöstö menetelmä teollisuudessa. Laser kaiverruksen etuja on tutkittu muun muassa aurinkokennojen tehokkuuden parantamisessa. Johtuen korkeista laatuvaatimuksista nopealle kaiverrusprosessille, on tärkeää monitoroida prosessia reaaliaikaisesti mahdollisten virheiden havaitsemiseksi prosessin aikana. Laser kaiverrusprosessin monitoroinnista tehdyistä tutkimuksista on kuitenkin puutetta. Yleisesti käytetyt monitorointi menetelmät muissa laser prosesseissa kuten laser hitsauksessa, ovat melko hitaita ja olemassa olevia sovelluksia ei voida toteuttaa laser kaiverruksen monitoroinnissa. Tämän diplomityön tarkoituksena on löytää menetelmä laser kaiverruksen monitorointiin suurnopeuskameran avulla ja arvioida monitorointi järjestelmän suorituskykyä sekä luotettavuutta kokeellisesti. Kokeissa käytetty laser laitteisto koostuu IPG ytterbium pulssilaserista 20 W:n maksimi keskiteholla ja Scanlabin Hurryscan 14 II laser skannerista f100 telesentrisellä linssillä. Kamera on kytketty skanneriin kamera-adapterin avulla, jotta prosessia pystytään seuraamaan. Kuvan käsittelyyn ja analysointiin on valittu tehokas täysin ohjelmoitavissa oleva teollisuustietokone. Virheen tunnistus algoritmit, jotka perustuvat partikkeli analyysiin, ovat kehitetty käyttäen LabVIEW -järjestelmän suunnittelu ohjelmaa. Algoritmin suorituskykyä on arvioitu analysoimalla paikallaan olevaa kuvaa laser kaiverruksesta resoluutiolla 960x20 pikseliä. Tuloksena maksimi analysointi nopeudeksi mitattiin 560 kuvaa sekunnissa. Algoritmin luotettavuutta arvioitiin kuvaamalla kaiverrus reittiä 2000 mm/s vaihtelemalla virheiden määrää laserin ollessa pois kytkettynä ja kuvan analysointi nopeuden ollessa 460 kuvaa sekunnissa. Koe onnistui ja tuloksena algoritmi tunnisti kaikki virheet kaiverrus reitiltä. Viimeinen monitorointi koe suoritettiin laser prosessin aikana. Haasteeksi osoittautui kuitenkin saada aktiivinen valaisu laser toimimaan laser skannerin kanssa, johtuen valaisulaserin linssin ja laser skannerin fyysisistä mitoista. Jotta virheen tunnistusta pystytään suorittamaan luotettavasti, valaisujärjestelmä tulisi vaihtaa.

ACKNOWLOEDGEMENTS

First, I would like to express my sincere gratitude to the examiners of my thesis, Professor Antti Salminen and D. Sc. Hamid Roozbahani for providing an opportunity to work in such the great project in the high-tech research lab with best possible equipment. Dr. Hamid Roozbahani has also given continuous supporting and direct guiding during the project, I am grateful from that.

I also express many thanks to my co-workers, Mika Ruutiainen and Veli-Matti Valtonen for giving great ideas to my work, Ilkka Poutiainen and Pertti Kokko for providing help with the building of test setup and Matti Manninen for guiding me in using of the laser.

Finally, I wish to give thanks to my friends for making my time in Skinnarila as enjoyable as it was and to my family as well as to my beautiful girlfriend for their sincere support during my studies.

Pekka Marttinen
Lappeenranta 16.5.2016

TABLE OF CONTENTS

LIST OF ABBREVIATIONS

CCD	charge-coupled device
CIGS	copper indium gallium selenide
CLIP	computational linguistics and information processing
CMOS	metal-oxide semiconductor
CPU	central processing unit
CW	continuous wave
DRAM	dynamic random access memory
DSP	digital signal processor
FPGA	field-programmable gate array
fps	frames per second
GMA	gas metal arc
HAZ	heat-affected zone
LabVIEW	Laboratory Virtual Instrument Engineering Workbench
PCI	peripheral component interconnect
ROI	region of interest
RT	real-time
UI	user interface
VI	virtual instrument

1 INTRODUCTION

Ultrafast lasers provide possibilities for many new microprocessing applications because of their capability for thermal ablation and their high peak power. One application is thin film laser scribing, which is used for example in solar panel technology for improving an efficiency of solar cells. In laser scribing applications, speed of the process can reach several meters per second, and quality requirements of the process are high. Disturbances in the process can cause defects to the scribing line, which affects the quality of the product. Currently, there is a lack of studies and solutions in process monitoring and quality control. Plenty of papers are published related to the more commonly used laser process applications in high power range such as laser welding. However, these processes are significantly slow compared to scribing process, and there is a need to develop a new monitoring system for fast laser scribing.

The aim of this study is to find out a method for monitor laser scribing process in real time utilizing a high-speed camera and detect possible defects from the process. In this case, defect means discontinuance in laser scribing. The speed of the laser scribing process sets high-performance requirements for real-time monitoring. An idea to perform the monitoring is to use a high-speed camera to scan the process and a fully programmable industrial computer to execute fast image processing and defect analysis. Software used for programming and developing the analysis algorithms is LabVIEW system design software. The purpose of this study is building a test setup for experiments and creating algorithms for the defect detection. One goal is also to find the maximum speed of analysis for the monitoring system. Reliability and performance of the monitoring system will be evaluated with practical experiments.

Before the building of the real-time (RT) monitoring system for laser scribing process inspection, some research is performed to find out how monitoring is implemented in case of laser welding process. In addition, some background study is performed to get needed knowledge from digital camera imaging, machine vision, and laser micromachining. After the theoretical part, building of test setup, experiments and experimental results are presented.

2   BASICS OF MACHINE VISION

According to Liu et al. (2015 p. 5) "Machine vision is defined as a process of integrating a variety of technologies and computational methods to provide imaging-based information. The scope of machine vision is broad, and it has been applied to a wide range of applications including robot guidance, quality assurance, sorting, material handling, optical gauging, automated assembly, industrial inspection." One important part of machine vision system is an image acquisition device. The purpose of the image acquisition device is receiving of illuminated light from optics and then converting the photon signal into electrical signal. This conversion is performed using an image sensor with electronics. When the combination is built to meet optical, electrical, mechanical and environmental requirements where it must operate, the combination can be called a camera. (Gilblom, 2012, p. 358.)

2.1   Digital camera sensors

Thousands of different camera models make selecting the right one for a specific purpose difficult. Information on cameras can be useful, but often too much information makes selection even more challenging. Understanding of some details of an image sensor is essential for evaluating a performance of the camera. (Gilblom, 2012, p. 448–449) Sensor types can be divided into two main types of image sensors, a Charge-Coupled Device (CCD) and a Complementary Metal-Oxide Semiconductor (CMOS) (Liu et al., 2015 p. 8–9). Teledyne Dalsa has compared these sensors in article CCD vs. CMOS "Neither is categorically superior to the other. In the last five years much has changed with both technologies, and the outlook for both technologies is vibrant. Both types of imagers convert light into electric charge and process it into electronic signals. In a CCD sensor, every pixel's charge is transferred through a very limited number of output nodes to be converted to voltage, buffered, and sent off chip as an analog signal. In a CMOS sensor, each pixel has its own charge-to-voltage conversion, and the sensor often also includes amplifiers, noise correction, and digitization circuits, so that chip outputs are digital bits." Advantages of the CCD and the CMOS are compared in table 1.

Table 1. Traditional view of Relative Advantages (mod. Apler, 2011).

CCD	CMOS
Image quality	High speed
Light sensitivity	On-Chip system integration
Read noise performance	Low cost of manufacturing
"Perfect" Global Shutter	High level of CMOS process Innovation

2.2 Camera interfaces

When building a vision system, the choice of the camera interface is one of the most important ones. It is important to consider different factors to find the optimum between performance, costs and reliability. Specifications of different camera interfaces are compared in table 2. (Fintel, 2013)

Table 2. Camera interfaces comparison (mod. Fintel, 2013).

Interface	Cable lengths	Bandwidth	Power over cable
USB 3.0	Up to 8 meters passive	350 MB/s net	Yes
Fire Wire	Up to 4,5 m	Max 64 MB/s	Yes
GigE	Up to 100 m passive	100 MB/s net	Yes
Camera Link	Up to 10 m for 85 MHz	Base 255 MB/s Medium 510 MB/s Full 850 MB/s	Yes

2.3 Digital camera imaging

The principle of CMOS designs is shown in figure 1. The CMOS sensor consists of an array of photodiodes, which are supplied with sampling and switching circuits. The simplest CMOS sensor resets the entire array of photodiodes by reverse biasing all diodes and then disconnects them from the reset voltage. When the exposure to light accumulates, the voltage across the photodiodes will fall immediately and image data can be produced from sampling voltages. Sampling is performed delivering the voltages from a row of

photodiodes to a bank of capacitors at the bottom of the sensor in order that these can be sequentially read out of the device by a column counter. A row counter selects the rows, which are wanted to be read. (Gilblom, 2012, p. 385.)
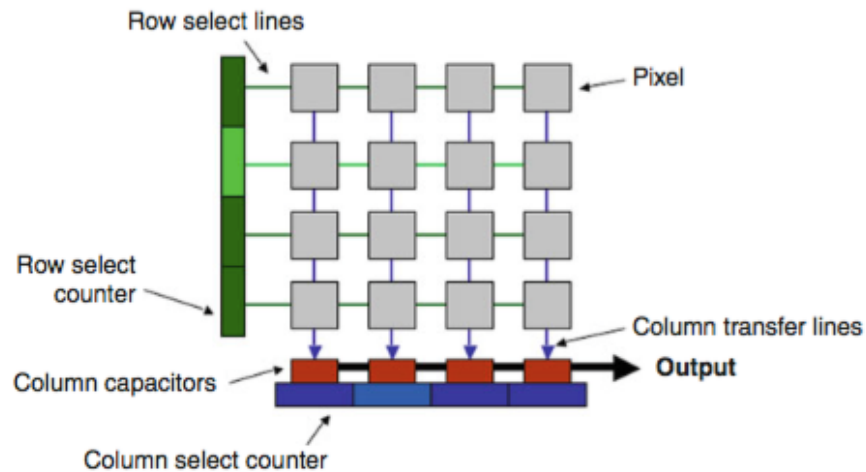
Figure 1. Principle of CMOS design (Gilblom, 2012, p. 385).

2.3.1 Scan control

Machine vision generally focuses on real-time operation where the timeliness of the whole process is critical. Real-time can be defined as the ability to provide the data extracted from the images in sufficient time for the processing task to be performed effectively. (Bailey, 2012, p. 1104) In general case such the television, a camera is operated with a periodic scan of the entire area of the sensor. Usually in industrial applications, simple periodic repetition scanning does not provide best results. Producing images on receipt of random of external commands is necessary for the camera. This is called triggering. (Gilblom, 2012, p. 389.)

Sometimes it is not needed to scan entire active area; instead concentrating on gathering data from particular part of the image provides benefits. This is called a region of interest (ROI) scanning, which is one way to speed up the frame rate. The advantage of CMOS sensors is that it allows define the scanning area, a number of rows to be scanned at once and a number of rows to be skipped before next scan by changing control parameters of the sensor. Generally, stopping the counter, which selects the rows for scanning, performs this modification. Similar controls can be used for the row of output capacitors in order that

only the columns of interest are allowed to continue to the output stage. By using these controls parallel, scanned area can be defined flexibly. (Gilblom, 2012, p. 388–389.)

Taps are additional outputs of image sensors. In addition to ROI scanning, using a multi-tap digital camera instead of a single-tap camera, image-acquiring speed can be increased by parallel readout of sections of the sensors. However, along the rows, the speed cannot be increased because the scanning of the taps executing in the same order on all taps. Only when the ROI is completely contained within one tap and the ROI is smaller than the number of columns, which are serviced by the tap, the speed can be improved. (Gilblom, 2012, p. 429–430.)

2.4   Commonly used image processing and analysis methods

According to Batchelor (2012, p. 701) "An image processing algorithm is a mathematical prescription for a computational process which describes the operation of part of the data-processing chain. (When we use the term "image processing algorithm" in connection with a vision system, we normally intend it to refer to the later stages in this chain, probably just the digital electron.)" The speed of the machine or image analysis application is essential. This term speed has two components, throughput rate and latency. Throughput rate means a number of the image processed or objects inspected during one-second time. Latency means time delay from the digitalization of an image to the achievements of results. (Batchelor, 2012, p. 702.)

2.4.1   Thresholding

Thresholding segments in an image into particle regions; analysis can be focused on areas that correspond significant structures. The operation is based on analysis of the pixel intensities. The resulting image from thresholding operation is a binary image. Thresholding often begins with many machine vision applications, for example, in particle analysis where the image is as first converted to a binary form for further image analysis. The principle of manual thresholding is based on threshold levels, which are lower and upper level. These levels define values for the pixels, which belong to particles in the sample frame. As an example from manual thresholding, there is a following source image shown in figure 3 (a) that is processed using threshold operations. Highlighting the pixels

within the threshold interval where the lower level is set to 166 and upper level to 255, the operation produces the image shown in figure 3 (b). (National Instruments, 2010a)

(a)　　　　　　　　　　　　　　(b)
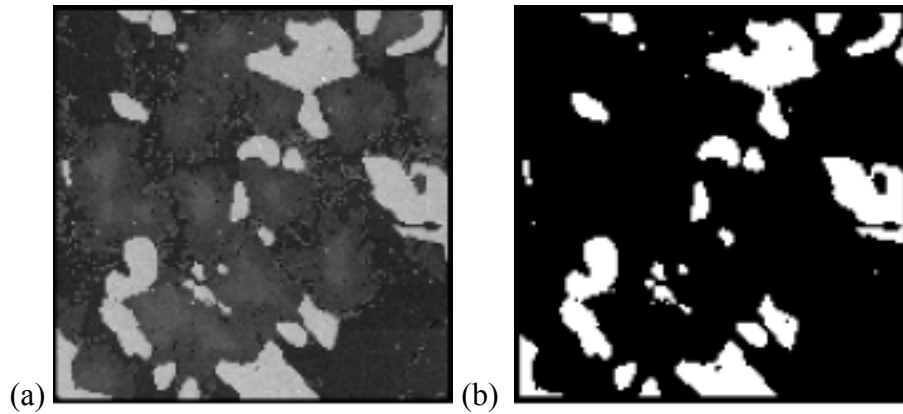
Figure 2. Source image of the threshold operation (a) and threshold image (b) (National Instruments, 2010a).

2.4.2　Edge detection

The principle of edge detection algorithm is finding differences in pixel intensities (edges) along a line of pixels in the frame under observation. The algorithm can be used for finding discontinuities in pixel intensities, which often illustrate the boundaries of objects in an image. The edge detection algorithm scans the pixel intensity pixel by pixel from the line. The principle is shown in figure 3 where the algorithm has analyzed the image from left to right, and the first edge of the region is marked in the picture. For proper and reliable image analysis utilizing edge detection algorithm, there are some requirements for the image quality. For example, too much noise in the image or poor contrast between the object and the background can lead to incorrect results. (National Instruments, 2010b.)

Figure 3. Edge detection algorithm scan example (National Instruments, 2010b).

2.4.3   Pattern matching

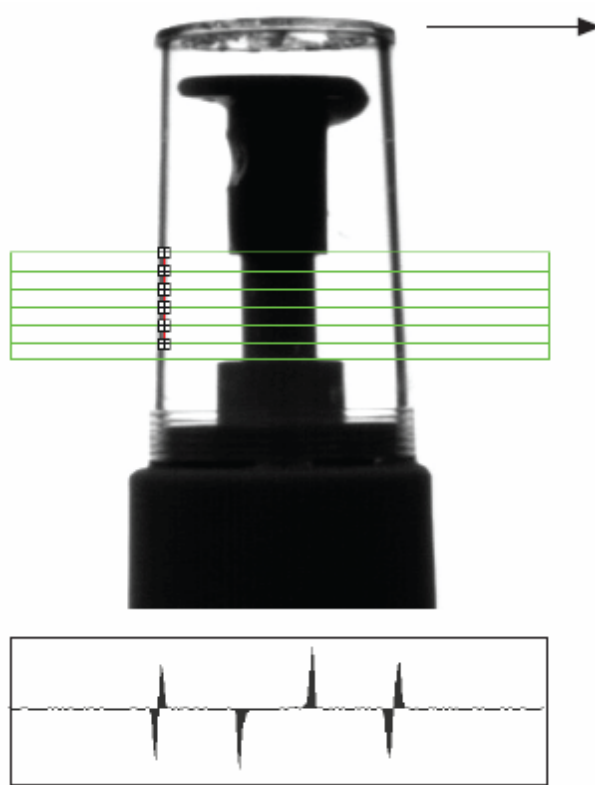Pattern matching finds parts from an image that match with the predefined reference pattern. When a template that represents the object for which are searched is created, the pattern-matching algorithm can find similarities from the pattern in acquired images and calculate a grade of similarity for the matches. Pattern matching is commonly used for determining the position or orientation of an object, measuring dimensions of a component, or detects errors, such as missing parts or poor print. For example, a printed circuit board can be searched for single or several fiducials. The pattern-matching algorithm utilizes the fiducials to get the board aligned for chip placement from a chip-mounting device. Part of the circuit board is shown in figure 4 (a). Figure 4 (b) shows a common fiducial, which is utilized in circuit board inspections or ship pick-and-place applications. The gauging algorithm first locates and then measure, the measurements of an object in an image. The object passes inspection only if the result is within the tolerance range, otherwise the object is rejected. (National Instruments, 2010c.)
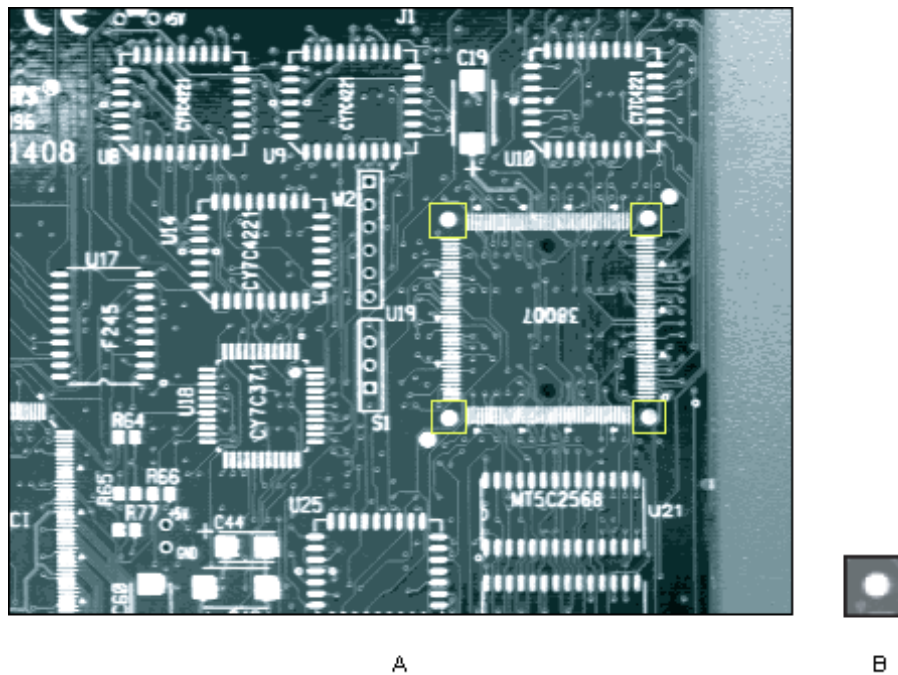
Figure 4. Circuit board and common fiducial for inspections (National Instruments, 2010c).

2.4.4   Particle analysis

Particle analysis is used for detecting connected regions of groupings of pixels from a frame under observation and then performs needed measurements of those regions, which are often related to particle. Particles are a continuous region of nonzero pixels. The analysis is based on series of image processing operations and image analysis actions, which give information about particles in an image. Particle analysis can be used for detecting and analyzing two-dimensional patterns from a frame. (National Instruments, 2010d.)

3   BASICS OF LASER SCRIBING PROCESSING

Lasers are widely used in industry for material processing, for example, cutting, drilling, piercing, and welding. Different laser types are developed for various purposes. Commonly used laser types are a gas laser, a solid-state laser, a free electron laser and a dye laser. (Steen & Mazumder, 2010, p. 32–50.)

3.1   Laser scribing and ultrafast laser material processing

Laser scribing is commonly used for forming kerfs, for example for separating semiconductors and ceramics. With some materials, maximum scribing speed can achieve several meters per second. Applications are found in the packaging industries, electronics, and photovoltaics. (Rofin.)

Some of the laser material processing applications set high requirements for material removal process and therefore ultrafast laser micromachining is required to be used instead of conventional laser processing methods. In conventional processing methods, such long-pulsed lasers, ablation of materials occur through melt expulsion driven by the vapor pressure and the recoil pressure of metal vapor. This process is unstable compared to ultrafast micromachining where ultrafast lasers, such picosecond (ps) or femtosecond (fs) is used. Figure 5 shows continuous wave (CW), nanosecond (ns), and (ps/fs) laser pulses. The black area in images illustrates the magnitude of the heat-affected zone (HAZ) and the blue lines illustrate the shock waves produced by the metal vapor. The CW laser creates largest HAZ because material is removed primarily by melting. In the case of ns laser pulses, material removing process is melt expulsion driven by the vapor pressure and the recoil pressure creating a smaller HAZ. As it can be seen from the image on the right, ultrafast pulses (ps/fs) create smallest HAZ or no HAZ at all, because material is vaporized away directly from the surface, resulting clean and smooth hole features and good process quality. (Lucas & Zhang, 2012.)
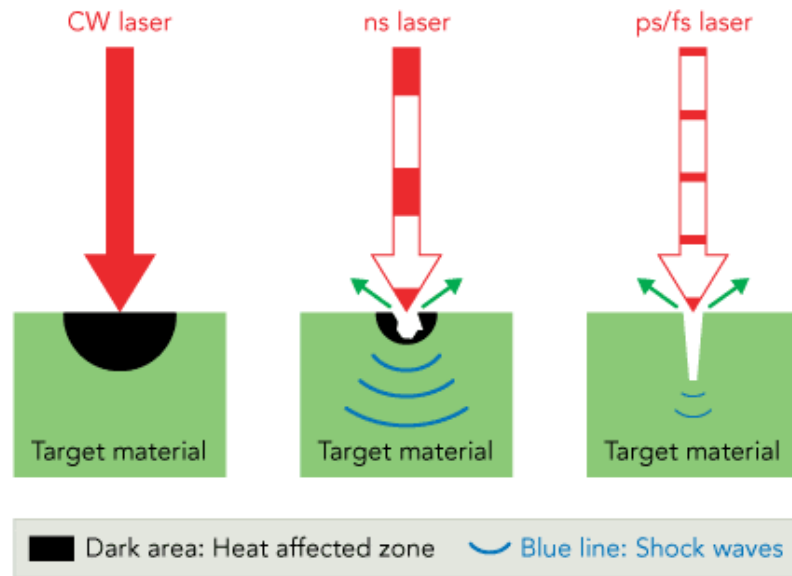
Figure 5. Laser material interaction basic for different types of lasers (Lucas & Zhang, 2012).

Some experimental results of glass processing are shown in figure 6 where the effect of laser pulse length to the hole features can be clearly noticed. The results from drilling and engraving experiments with nanosecond laser are shown on the left side and the results with femtosecond laser are shown on the right side in figure. Femtosecond laser represents more than two million times shorter pulse duration, resulting shaper hole features. (Lucas & Zhang, 2012.)
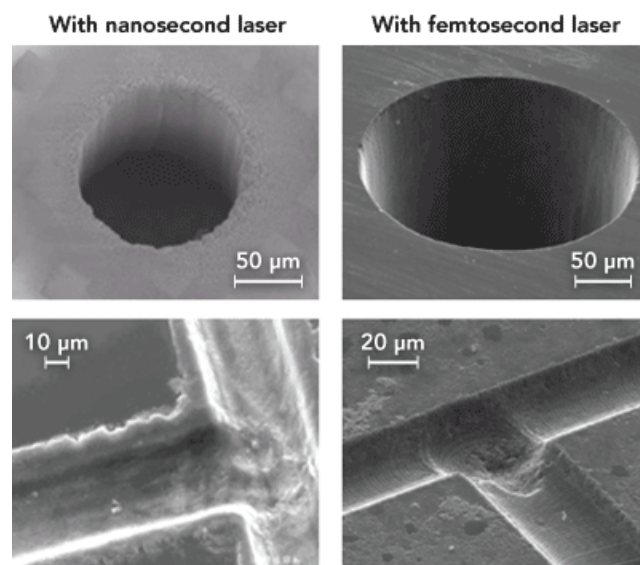
Figure 6. Images from laser processing experiment on glass with a ns-laser (left-side) and with a femtosecond laser (right-side) (Lucas & Zhang, 2012).

3.2   Ultrafast lasers applications for solar panel manufacturing

Copper indium gallium selenide (CIGS) is rapidly growing choice as a material for thin-film photovoltaics as a result of its good efficiency. There have been problems to implement laser scribing in CIGS solar modules manufacturing. Therefore, mechanical scribing with a force-controlled stylus has been commonly used manufacturing method. However, the mechanical method has also own problems, example poor edge quality and more importantly, irregularity in scribing lines that demand wide spacing between adjacent scribing lines. (Rekow et al., 2010 p. 1.) As a result, changing scribing method from mechanical scribing to laser scribing, the efficiency of the module is possible to be increased up to four percent (Eberhardt et al., 2010). According to Burn et al. (2015) "Specific laser processes selectively remove layers between deposition processes; thereby creating monolithic cell- to-cell interconnections with a very small loss of productive area. Ultrashort pulsed lasers are the tool of choice for scribing Cu(In,Ga)Se 2 (CIGS) thin-film solar cells as they provide the necessary process selectivity and minimize thermal load on the surrounding material."

4   EXISTED HIGH-SPEED CAMERA MONITORING APPLICATIONS FOR LASER PROCESSES

Utilizing of machine vision applications in laser process monitoring is widely studied. The purpose of the monitoring is gathering information from the process and using that information in developing of quality control methods. A lot of monitoring applications are provided for laser welding process monitoring and during several years, also closed-loop systems are demonstrated. Advanced digital camera and data processing technology have provided possibility to develop systems based on feature recognition for determining certain features of the process. (Purtonen et al., 2014.)

When the processing parameters are not controlled by real-time monitoring signal, the monitoring system is called an open-loop system. In the open loop system, the process is not adjusted according to the output signal, but the only signal is created which indicates that there is an error in the process. Because quality and reliability of the process is important to be ensured, in recent years the closed loop manufacturing systems have become more popular. Formerly only simple sensors, such photodiodes are used in closed loop systems, but recently a digital camera technology is improved and they are more commonly used as detectors. Such systems can be used for example for measuring changes in keyhole shape and size or melt pool shape in the laser process and the feedback signal from the camera can be used for controlling process parameters. (Purtonen et al., 2014, p. 1223.)

4.1   High-speed camera applications for laser welding monitoring

According Tenner et al. (2015, p. 1) "Laser welding offers great flexibility and a high degree of automation. The process is highly dynamic and consists of complex multidimensional mechanisms that can lead to weld defects. Furthermore, the time span in which defects evolve (likely to be less than 1ms) makes it hard to fully control the process and anticipate the formation of joint defects." However, according to experimental results the radiation from the plasma or metal vapor plume in the laser material process can be analysed and the results can be used in the quality analysis. Also, it has been noticed that the melt pool behaviour gives useful information from the laser welding process. (Purtonen

et al., 2014, p. 1227.) Fennander et al. (2009) have studied analysis of regularity of the arc frequency and the flight direction of a droplet in a hybrid welding process. These factors are important because the regularity of the frequency affects the welding quality and also flying direction of the droplet can affect the quality because if the droplet flights straight to the laser beam or the keyhole, the droplet blocks the laser, causing incomplete penetration of the beam to the workpiece.

Commonly used feature point detection algorithms for welding monitoring are pattern recognition, Hough Transform, and line fitting. However, all these algorithms are computationally intensive, which sets the limits for the performance of the inspection system. Pattern recognition uses predefined templates for comparing acquired image data from the process and predefined templates. In that case, involvement of convolution operation noticeably increases the computation load. Computation load is a problem also with Hough Transform and line fitting algorithms because they are two-step processes. For detecting corner point's of the weld joint, first the weld joint profile has to be identified and then the feature points are able to be found from the image. (Huang & Kovacevic, 2012.)

Chen et al. (2009) have studied closed loop control of welding robot. The control loop is based on analysis of welding penetration depth and melt pool size with CCD camera imaging. Welding quality has been analyzed using canny operation, which is edge detection based image analysis method. Welding robot has been controlled according to results from image analysis. Total image processing time is 155 ms. (Chen et al. 2009, p. 567-576) In the year 2013 method for diagnosing gas metal arc welding (GMA) process, based on the analysis of fused infrared and vision images of a welding arc is presented. The FireWire interface is used for connecting the cameras to the server. Software for image acquisition and camera synchronization is developed in LabVIEW environment. In this study, first ROI has been selected from the image and then different pattern recognition algorithms have been performed to analyze welding process for selecting optimal one. Image analysis speed in experiments has been 50 frames per second (fps). (Fidali & Jamrozik, 2013, p. 242–251.)

One solution for faster welding monitoring and process control is laser-based machine vision system. Camera used for image acquiring is a Gigabit Ethernet high-speed camera using a monochromatic sensor with 659 x 494 array of 8-bit pixels. LabVIEW system design software has been used for developing algorithms for image processing and analysis. The principle is following the profile of the welding joint with laser stripe and imaging the stripe with the embedded CMOS sensor. The sensor has been directed to gather reflected light from the laser stripe and shape of the stripe in images gives information from the laser profile of the welded joint. Most important factor that sets the limit for the performance of the monitoring system is the efficiency of the image-processing algorithm, which analyses position information and geometrical features of the welding joint. The maximum image analysis speed for the algorithm is about 300 fps. (Huang & Kovacevic, 2012.)

5 TEST SETUP

Test setup for experiments including laser, scan head, illumination, camera and camera adapter is shown in figure 7. Further explanation of the hardware and software used in experiments is presented in the following sub-sections.
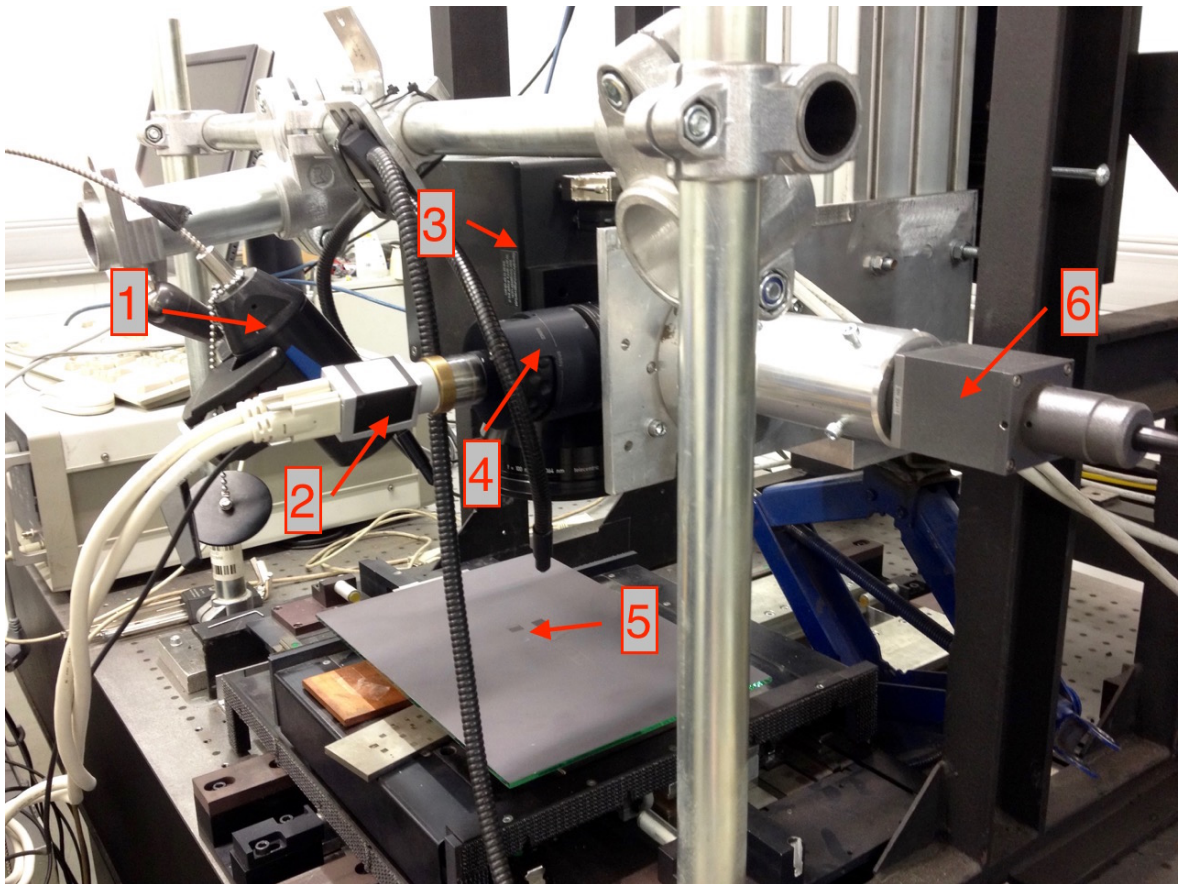
Figure 7. Test bed for experiments (1. Illumination laser, 2. High-speed camera, 3. Scan head, 4. Camera adapter, 5. Work piece, 6. Pulsed fiber laser).

5.1 Pulse laser

The laser used in the experiments is an IPG ytterbium pulsed fiber laser with 20 W maximum average power, typical beam quality M2 value of 1.5, 1 mJ max pulse energy, 1.6-1000 kHz pulse repetition rate, and a changeable pulse length from 4 ns to 200 ns in 8 increments. Scan head optics used in the laser is Scanlab's Hurryscan 14 II with an f100 tele-centric lens. Working area is 54x54 mm^2 and the laser spot size at minimum 28 μm but realistically closer to 40 μm since it is difficult to keep the laser beam in exact focus with

the current setup. Used laser control software is SamLight version 3.0.5 build-0582 by Scaps GmbH.

5.2 Camera Adapter

The camera adapter is chosen from Scanlab. It is installed between the scan head and laser flange, allowing the camera to follow laser beam and capturing continuous image from a surface processed by the laser. Technical information of the adapter is presented in table 1 and drawings of the camera adapter are shown in appendix I.

Table 3. Technical information of the camera adapter.

Diameter of entering beam	Max 30 mm
Connection type for camera Maximum chip size of camera	C-Mount 2/3"
Weight (Without camera)	Approximately 1.6 kg
Operation temperature	25 °C ± 10 °C

5.2.1 Principle of Operation

A dichroic beam splitter inside of the camera adapter passes through the laser beam from the laser source to the working surface, but the back-reflected light from the illuminated surface is decoupled for the camera. The laser beam passes through the beam splitter practically unaffected, the power loss being from 0.5 to 1 percent when the lens is clean. The sharpness of the image is adjusted from the objective unit's focus ring.

5.2.2 Observation Field and Resolution

The focal length of the scanning objective and chip's size of the camera defines the size of the observation field. For an example, focal length of 163 mm with 2/3 inch censor size, typically produces an image field size of approximately 7.5 mm x 10 mm, maximum optical resolution beings around 10 μm.

5.3 High-speed Camera

The high-speed camera chosen for the project is Basler acA2000-340km. It is a grey scale Camera Link camera for high-speed imaging in real time. Specifications of the camera are presented in table 2, and measurements are presented in appendix I.

Table 4 High-speed camera specifications (mod. Basler).

Full resolution (width x height)	2048 x 1088 Pixel
Pixel size (horizontal/vertical)	5.5 x 5.5 μm^2
Maximum frame rate with full resolution	340 fps
Pixel bit depth	8, 10 and 12 bit
Camera Link clock	32.5 / 48 / 65 / 82 MHz
Lens mount	C-mount
Power consumption (typical)	3.0 W
Weight	96 g
Sensor vendor	CMOSIS
Sensor type	CMOS
Sensor size	11.26 mm x 5.98 mm
Maximum image circle	2/3 inch

5.3.1 Camera triggering

The software of an illumination system controls the camera trigger. The trigger signal is TTL 5 V and it is delivered from the illumination system to the Camera Link modules D-SUB port where it is delivered forward to the camera via the Camera Link cable. The camera operates as the slave and the illumination software operates as the master.

5.4 Illumination system

Lighting produced by illumination system is essential for machine vision applications. An illuminated workpiece reflects the light of the lightning source to the camera ship, which collects the light and builds the image for further image processing and analysis. (Liu et al. 2015)

The illumination system used in the laser process monitoring experiments is a high-frequency pulsed diode laser light source Cavilux HF (figure 8) with 500 W maximum

output power. Illumination operates at a wavelength 810 nm. It is used for visualization of high speed and high-temperature processes. High temperatures in laser process produce bright vapor cloud. Without the illumination system, it is impossible to capture accurate images through the brightness. Brightness is filtered out from the image using bandpass filter before sensor of the camera, which passes through only reflected light from illumination laser.

Figure 8. CAVILUX HF illumination system (1. Controller, 2. Laser lens, 3. Laser unit).

5.5   Industrial computer (PXI-system)

PXI is open PC-based platform created by National Instrument for test, measurement and control systems. PXI deployment platform is used example in applications such as manufacturing test, machine monitoring, and industrial test.

The PXI system shown in figure 9 is built for the experiments consists of NI 1483 Cameral Link Adapter Module, NI PXIe 7966R FPGA Module and NI PXIe-8880 Real-Time Module. The modules are presented in the following subsections.
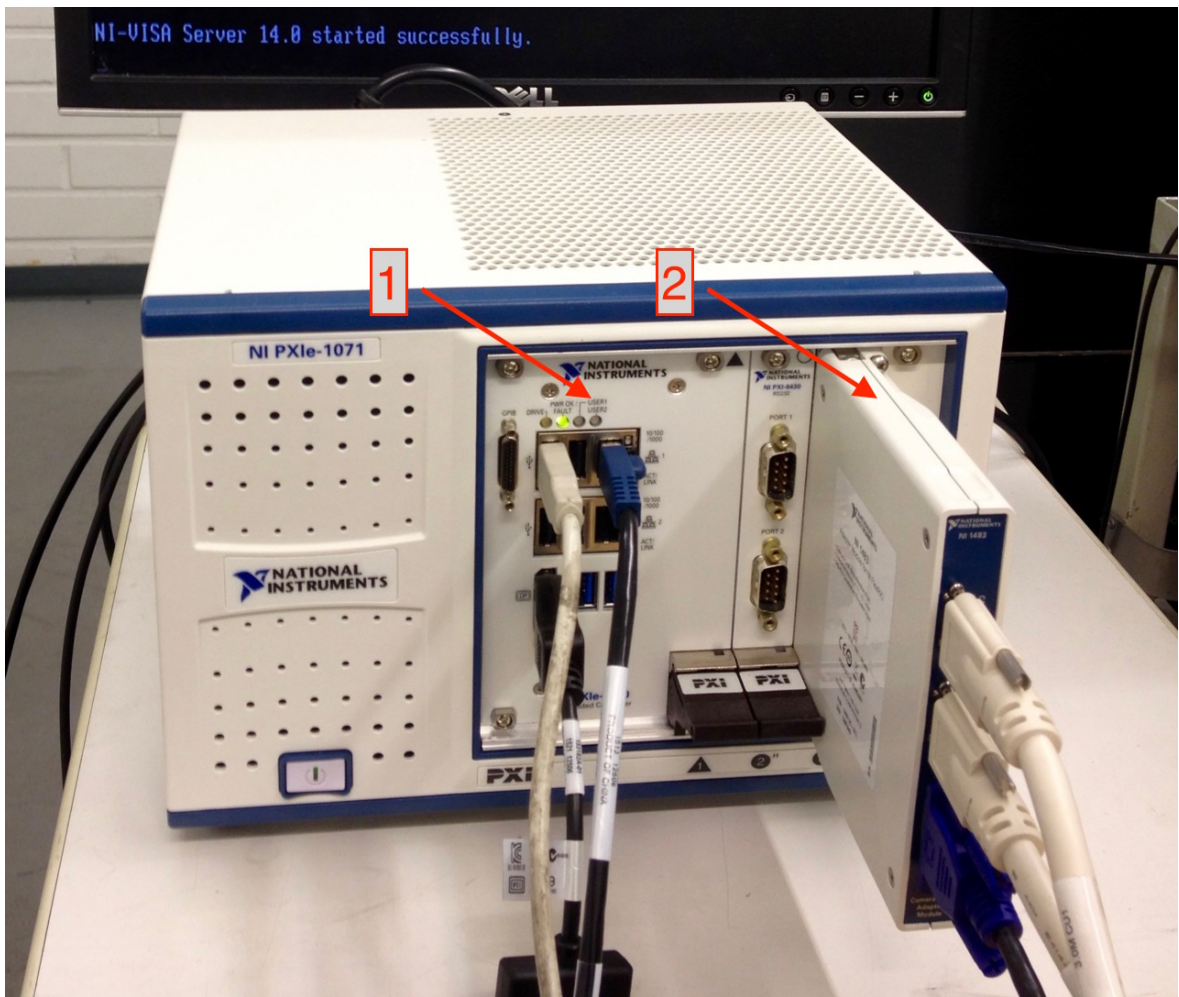
Figure 9. PXI System (1. RT-Controller, 2. Camera Link module connected to FPGA module).

5.5.1   PXIe Real Time module

The NI PXIe-8880 is an embedded controller that utilized Intel Xeon CPUs (Central Processing Unit) for fast calculation in different test engineering applications. It is equipped with eight-core processor enabling low latency in calculation. That makes it suitable for high-speed real time image processing applications.

5.5.2   NI FlexRIO FPGA module

NI FlexRIO hardware is customizable input/output module developed to operate with NI LabVIEW FPGA (field-programmable gate array) modules. It is consisted of from two parts, which are NI FlexRIO (FPGA) module and NI FlexRIO adapter module. NI FlexRIO FPGA module is reconfigurable with LabVIEW system design software.

The NI PXIe-7966R FPGA module features a DSP-focused Virtex-5 SX95T FPGA and 512 MB of on-board DDR2 DRAM (Dynamic Random Access Memory). This FPGA incorporates 640 Digital Signal Processor (DSP) slices that it can be used to implement digital filters, custom signal processing and fast Fourier transform logic, all of which are commonly found on analog FPGA-based instruments. Also, the theoretical on board DRAM throughput of 3.2 GB/s is necessary when operating on large data sets with the highest-performance adapter modules.

5.5.3   Camera Link Adapter Module

The NI 1483 is a Camera Link adapter module for Cameras, which use Camera Link interface. It operates together with NI FlexRIO FPGA modules, supporting 80-bit image data and 10-tap parallel pixel acquisition utilizing base-, medium-, or full Camera Link configuration. It is equipped also with digital I/O channels. Channel one and two are optically isolated inputs and channel three is quadrature encoder input, which can be used for external triggering. The Camera Link adapter module is paired with the FPGA module to execute custom image analysis. By implementing the process in hardware, FPGA processing does not use CPU power from the PC or controller. Frames acquired to the FPGA module via Camera Link adapter, can be processed independently or with RT-controllers CPU.

5.6   LabVIEW System Design Software

LabVIEW (Laboratory Virtual Instrument Engineering Workbench) system design software is used for developing applications in science as well as in engineering. It differs from standard C or Java designing systems because it uses a graphically based programming language to build programs in pictorial form.

A program developed with LabVIEW consists of virtual instruments (VIs). Vis appearance and function often simulate physical instruments. Vis consists of the block diagram and the front panel, where the block diagram is the VI's source code, and the front panel is the interactive user interface. Physical instruments are simulated in the front panel, where user inputs and indicator are presented with push buttons, knobs, displays, and many other controls.

6 IMAGE ACQUISITION, PROCESSING AND ANALYSIS ALGORITHMS

Referring to the study in theoretical part of this paper, the image analysis methods used in welding monitoring are computationally intensive and significantly slow. Example monitoring applications based on pattern recognition techniques, analysis speed is around 50 fps due complexity of the algorithms. For monitoring laser scribing process, the speed is needed to be increased.

In this study, the purpose of the laser scribing monitoring is finding discontinuities from the scribing process. Because the purpose is not analyzing process any another way than sort out is laser scribing line coherent or not, the analysis algorithm can be simpler than algorithms used in welding monitoring. Utilizing the study about defect analysis methods and results of several experiments, a method based on particle analysis is chosen for the experiments. Another viable option was edge detection, where pixel value differences were observed from scribing line. However in simple experiments, it was found that algorithm is unreliable if image quality is poor or noisy due example of bad illumination. Therefore, particle analysis method seems to be a potential option for executing the analysis efficiently.

Image acquisition, processing, and analysis procedure follow the pattern presented in figure 10. The algorithms are presented more briefly in following subsections. Different components of the algorithms shown in the figures are numbered, and the equivalent numbers in the text explains functions of the particular components.
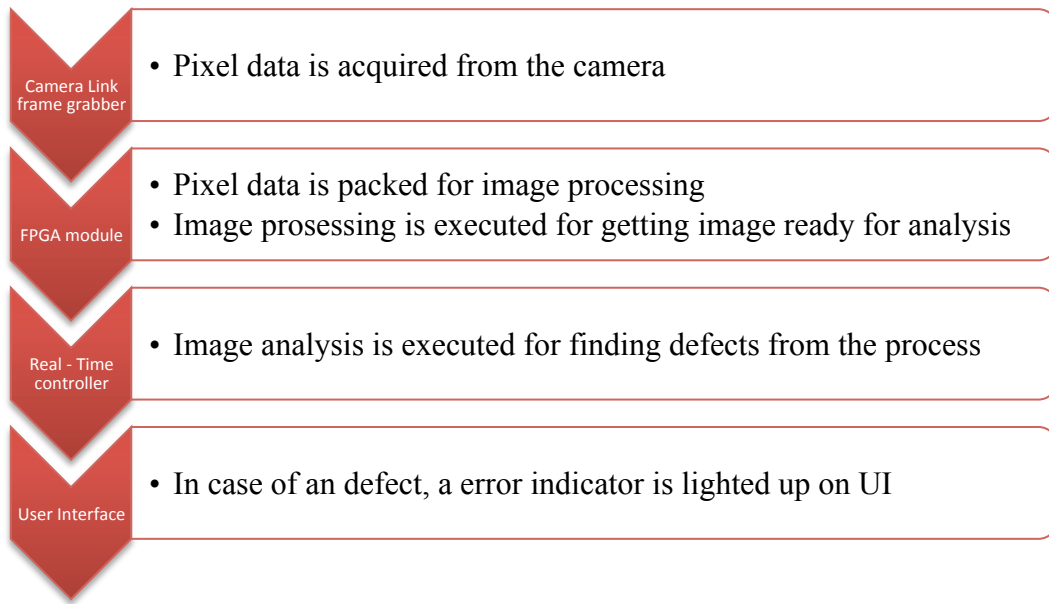
Figure 10. Image processing and analysis procedure.

6.1 Image acquisition on FPGA

Block diagram presenting pixel data acquisition and acquisition state machine is shown in figure 11. Data from the camera is delivered to Camera Link-module through Camera Link cables. The first phase is organizing acquired Camera Link data output into pixels (1). Then the pixels are written into small FIFOs (named Cam Data 16 and Cam Data 64) (2), which provide small buffering for DRAM write delays. Image acquisition is controlled by acquisition state machine (3). The purpose is acquiring the image from the camera only when the image is ready for acquisition. For fast image acquisition, camera parameters are set to 10-tap mode, allowing ten pixels parallel acquisition. When the camera is ready for pixel data sending, the acquisition state machine sends a command for the acquisition FIFOs to starting data acquisition. The acquisition state machine also provides information about image frame acquisition, such the number of frames acquired, the number of line per frame (image width) and the number of clocks per line (image height). The information from the acquisition state machine is sent to the user interface (UI) as well as acquisition status information for informing the user when the acquisition is in progress.
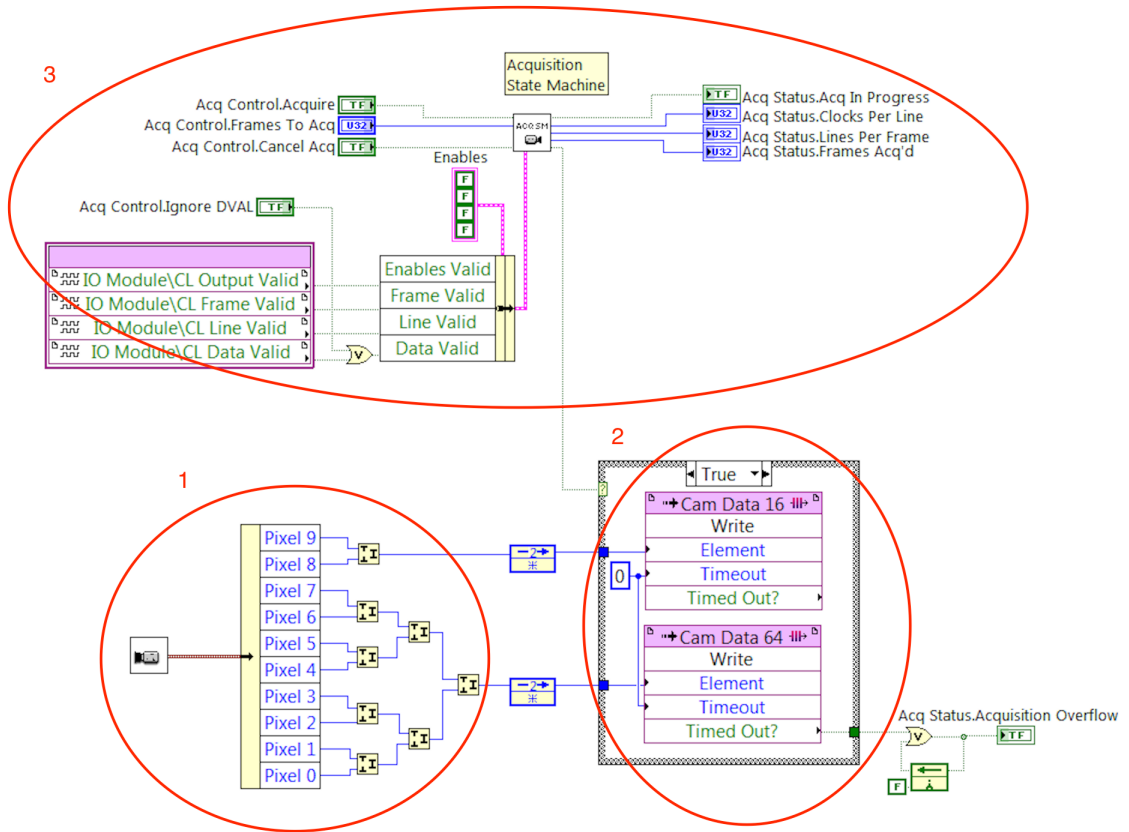
Figure 11. Pixel data acquiring and acquisition state machine.

The data transfer from Cam Data FIFOs to packer CLIP is shown in figure 12. The data is read from the Cam Data FIFOs (4), and the data is written to a packer CLIP (Computational Linguistics and Information Processing) (5). The packer takes the 80-bit camera data and packs it efficiently into 256-bit words that it can be written to the DRAM FIFOs.
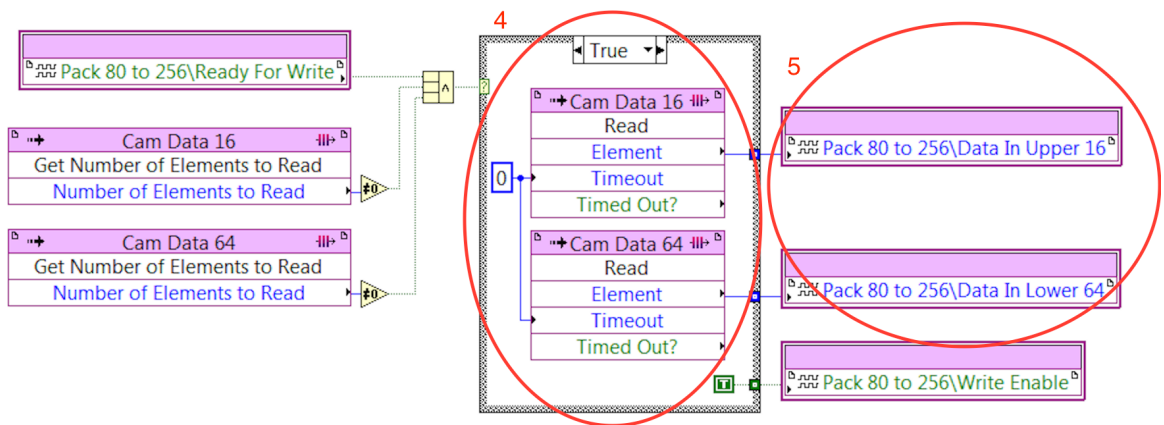

Figure 12. The data transfer from Cam Data FIFOs to packer CLIP.

256-bit data is transferred from the packer (6) to DRAM (7), which serves as a very large frame buffer. Block diagram is shown in figure 13.
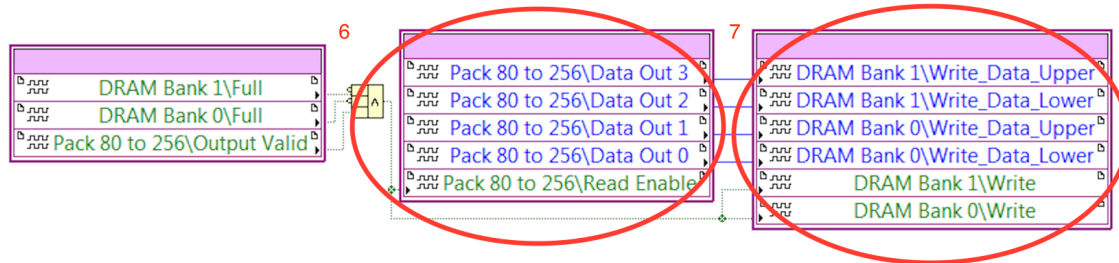

Figure 13. The 256-bit data transfer to the DRAM.

The data is read from the DRAM (8) and transferred to another packer (9). This packer takes the 256-bit data from DRAM and packs it into 64-bit words. Bock diagram is shown in figure 14.
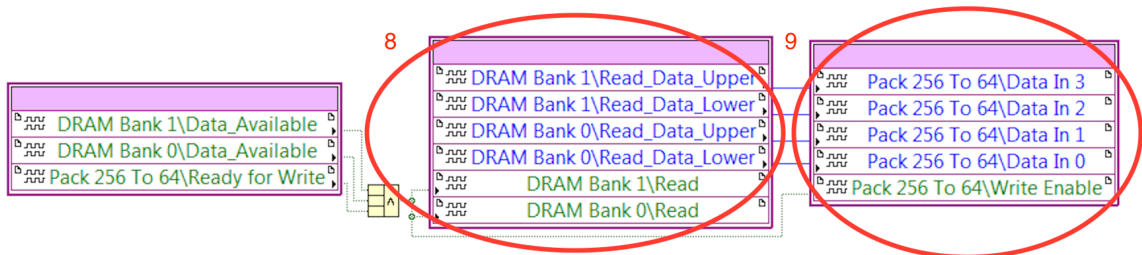
Figure 14. The data packing from 256-bit to 64-bit words.

6.2   Image processing on FPGA

The 64-bit data is transferred and divided from packer (10) to eight different FIFOs (11). One of these FIFOs is shown in figure 15. The FIFOs provides small buffering for thresholding operations. The 8-bit data is read from acquisition FIFOs (12) and converted into Pixel Bus format (13) for thresholding operations (14). After thresholding, threshold image data is written to Host FIFOs (15) for the data transfer from FPGA to Real-time (RT) controller.
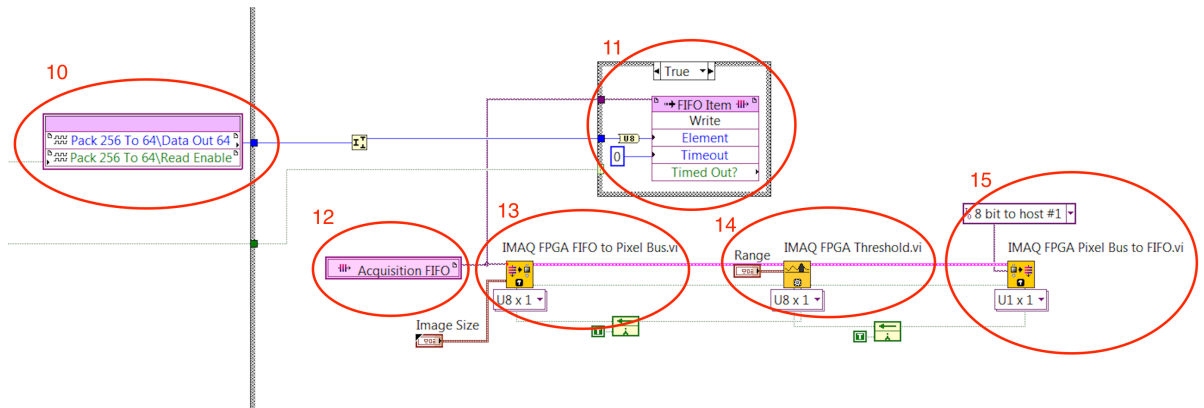
Figure 15. Image processing algorithm

6.3 Defect detection on RT-controller

The 8-bit threshold array data is read from the Host FIFOs (16). Array data from eight FIFOs is converted to image data (17) for the image display and image analysis algorithms. In the case of image data is written to FIFOs faster than data is read out from FIFOs, a number of data elements left to buffer is sent to UI (18). Possible reason for that could be for an example if image analysis is not able to analyze as much data as is acquired from the camera and the buffers of the FIFOs starts to fill. FIFOs are shown in figure 16.
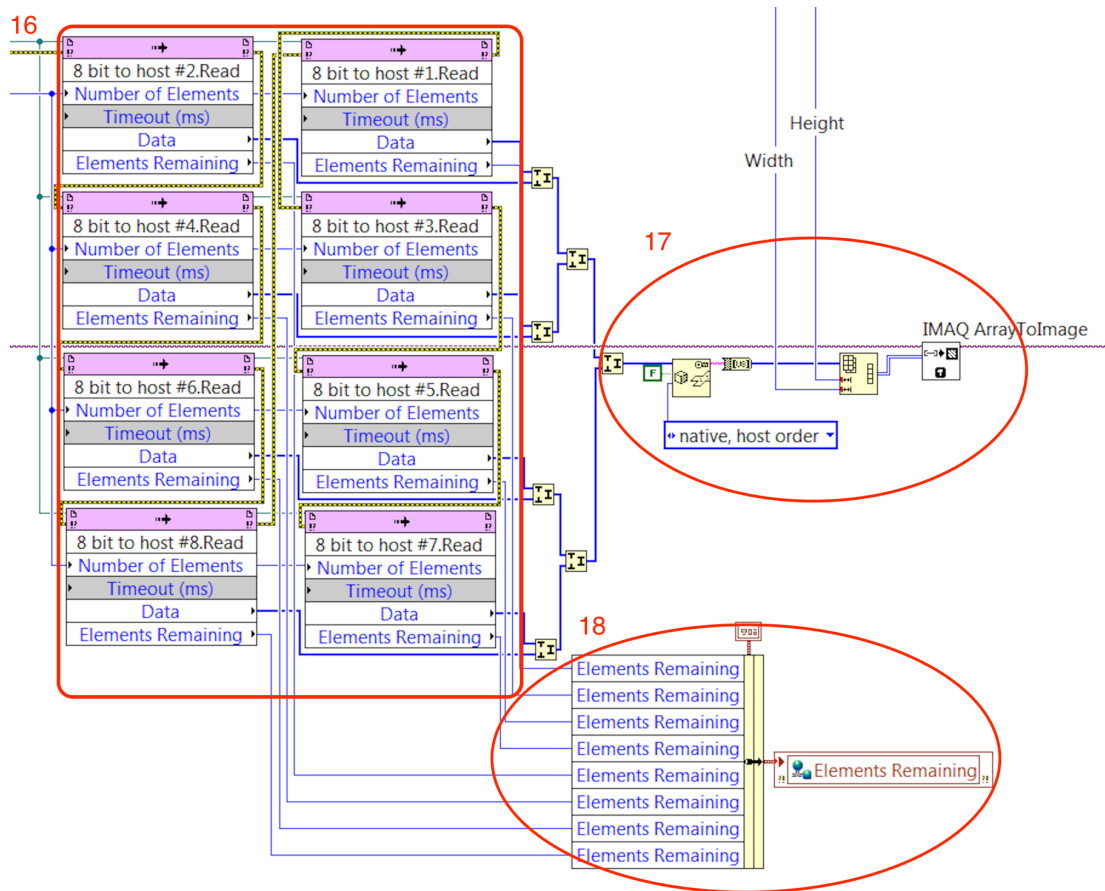
Figure 16. Array data conversion to image data.

The first phase in image analysis is removing small-unwanted particles from the image (19). Then the image is ready for particle analysis (20). Particle analysis calculates numbers of particles from the image and returns the value to the UI. In the case of defect, error information is sent to UI (21). In addition, a number of errors are calculated using increment inside of case structure, which is added to indicator in every iteration. Data flow is shown in figure 17.

Figure 17. Image analysis algorithm.

6.4   User interface

User interface runs on PC. Data from the RT-controller to the PC and vice versa is delivered via Ethernet connection between the PXI-system and the PC. The connection is performed using shared variables.
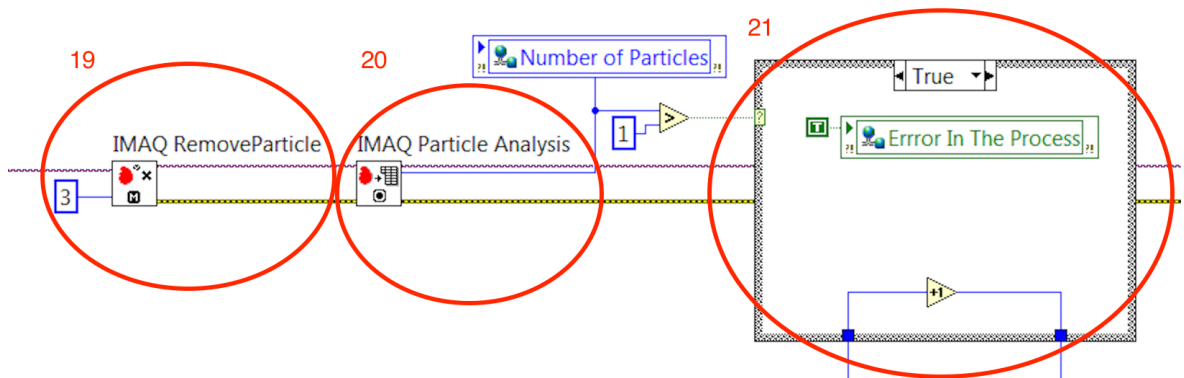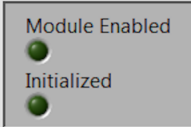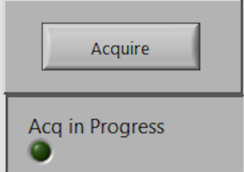
The PC VI's UI guides a user through the process, which is divided into four different phases. Phases are shown in figure 18. (1) The first phase is running VIs and checking form indicator that the camera clock is found, and Camera Link module is ready. (2) The second phase is set the camera ready for image acquiring. When the "Acq in Progress" light is lighted up, the camera is ready and is waiting for the trigger. (3) The third phase is adjusting the camera exposure time and threshold range. In addition, the camera can be focused and directed as desired and illumination can be set. A software trigger can be used instead of external trigger to acquire a single image from the camera and acquired images are shown on display on the RT VI's UI. (4) Starting the process monitoring is the last phase. Error information (number of particles and number of defects) is delivered from the RT-controller to the UI and image acquisition information (number of frames acquired, frame height, frame width and the number of frames acquired in second) is shown on UI (figure 19). Status of FIFOs buffers is also indicated for informing the user in case of image overflow in FIFOs.
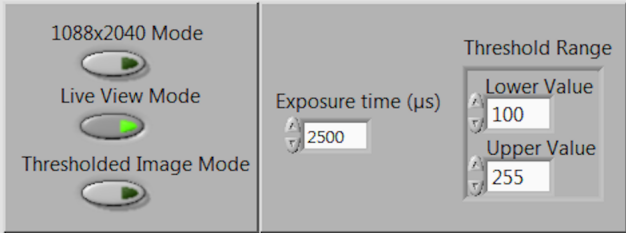
1 1. - Run the RT and the PC VIs
 - If the PXI-system and the camera is connected properly and turned on, the "module enabled" and the "intialized" indicators is lighted up for indicating that the CL module is ready for acquisition and the camera clokc is detected.

Module Enabled

Initialized

2 2. - Press the "Acquire" button.
 - When the camera is ready for image acquiring,
   the "Acq in Progress" indicator is lighted up and the camera is wating for the frame trigger.

Acquire

Acq in Progress

3 3. - Use the Live View Mode to see image from the camera. It is useful for setting up camera parameters.
 - By selcting 1088x2040 Mode, larger surface can be seen when "user set 1"* is selected from the camera.
 - Treshold Image Mode can be used to see thresholded image when the Live View Mode is turned off.
 - When the camera and threshold range is set, turn "1088x2040" -, "Live View" - and "Thresholded image" -modes off
   before starting process monitoring.
RERUN VIs ALWAYS AFTER THE MODE IS CHANGED!

1088x2040 Mode

Live View Mode

Thresholded Image Mode

Exposure time (µs)
2500

Threshold Range
Lower Value
100
Upper Value
255

*User sets of the camera
- User set 1: 2040x1088 pixel
- User set 2: 960x40 pixel

Software trigger can be usefull for setting up the camera

Send Software Trigger
Send pulse
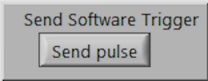
Figure 18. Controls on PC's user interface.

4. - Start process monitoring by strarting triggering the camera.
   - Indicators panel shows number of acquired frames,
     frames acquired per second (FPS), number of particles detected in real time and
     numbere of defects deteccted during a process.
   - Monitor FIFOs for case of overflows.

4

Indicators	Acquisition FIFOs
Frames Acq'd	Elements Remaining 1
0	0
Acq'd Frame Height	Elements Remaining 2
0	0
Acq'd Frame Widht	Elements Remaining 3
0	0
Fps	Elements Remaining 4
0	0
Number of particles	Elements Remaining 5
0	0
Number of defects detected	Elements Remaining 6
0	0
	Elements Remaining 7
Defect Detected	0
	Elements Remaining 8
	0
	64 bit FIFO overflow

Figure 19. Indicators on PC's user interface.

7   EXPERIMENTS

For evaluating reliability and performance of the built monitoring system, experiments are performed in four phases. The different phases are shown in figure 20, and they are explained more briefly in following sub sections.
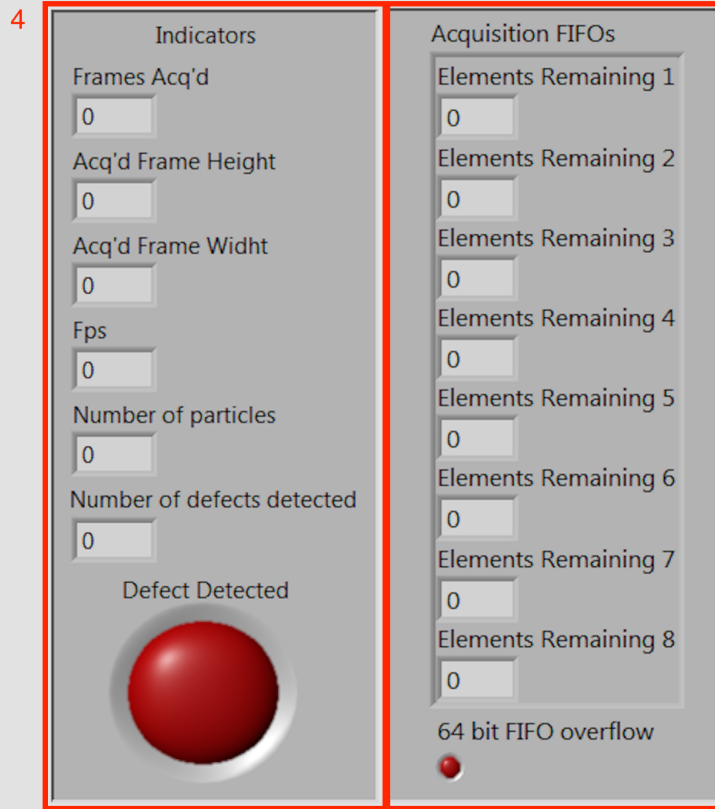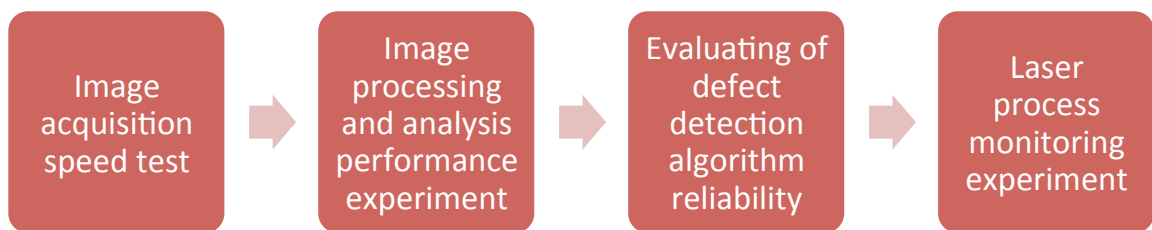
Image acquisition speed test	→	Image processing and analysis performance experiment	→	Evaluating of defect detection algorithm reliability	→	Laser process monitoring experiment

Figure 20. Experimental phases.

7.1   Image acquisition speed test

Acquisition speed test can be performed disconnecting analysis algorithms and displays from the process. When only acquisition algorithms are run without any other components in the code, maximum image acquiring speed (frame rate) can be defined by increasing triggering frequency until camera do not acquire frames any faster.

7.2   Image processing and analysis algorithms and performance experiment

Before the particle analysis can be performed, a grey scale image has to be changed to a binary worm using thresholding operations. There is a corresponding value of the light intensity between 0 and 255 for each pixel, when the lowest light intensity returns value 0 and the highest light intensity returns value 255. By selecting threshold levels within this range, interested information form the image can be highlighted. The thresholding operation returns value 1 for bright pixels and value 0 for dark pixels. Value 1 is shown as a white and value 0 as a black in the images.

When the image is in the binary worm, it is possible to count particles form the image using particle analysis algorithms. Before the analysis, a region of interest (ROI) should be chosen from the binary image. In this particular setup, width of the measured observation area is 10 mm and length of the scribing line in frame is 4.7 mm. The length of the scribing line is about half of the observation area because laser spot is middle of the area. The ROI is shown in figure 21, which is defined manually from the image using pixel calculator. The particle analysis is executed only inside of that area. Principle of the analysis is based on the number of the particles. When the scribing line is coherent, there is only one particle inside of the ROI and if there is discontinuous (defect) in scribing, the ROI includes at least two particles.

Figure 21. Selection of the ROI.

Impurity on the surface can create small particles into the ROI. These small particles can distort the result of the defect analysis. Therefore, the particles have to be removed before the analysis. These operations can be performed using an advanced morphology operations in LabVIEW. Figure 22 shows the image after the threshold operation. Small-unwanted particles inside the ROI could be seen in the figure (one of them are zoomed). Unwanted particles should be removed from the image before the particle analysis. The minimum particle size is set to 3x3 pixel, and all smaller particles are removed. Figure 23 shows a binary image without unwanted particles.
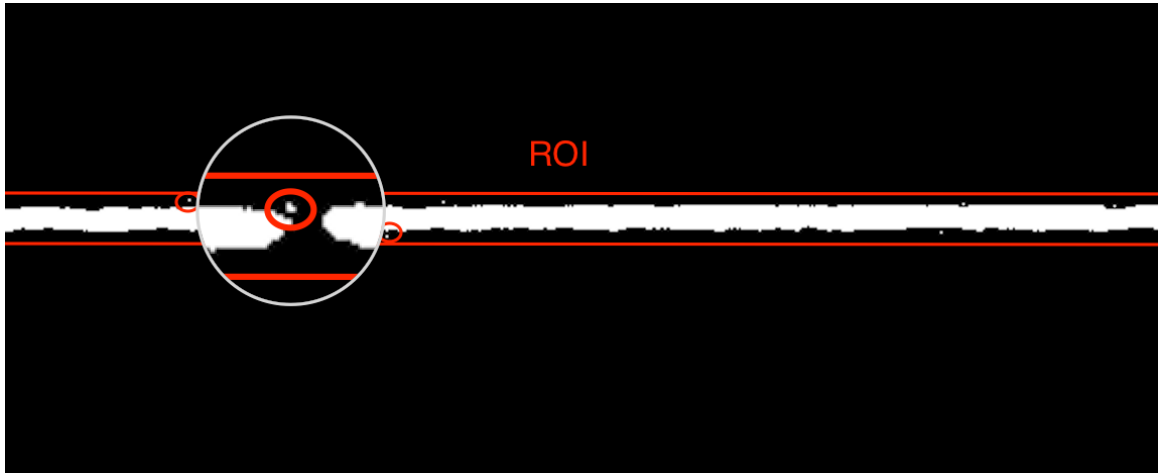
Figure 22. Threshold image with unwanted particles.

Figure 23. Threshold image where unwanted particles are removed.

As it can be seen from figure 24, after the morphology operations, there are two particles inside of the ROI. All unwanted particles are removed, and the image is ready for the particle analysis. As a result, the analysis returns number of the particles and in this particular case, the defect can be detected because the image includes two particles instead of one.

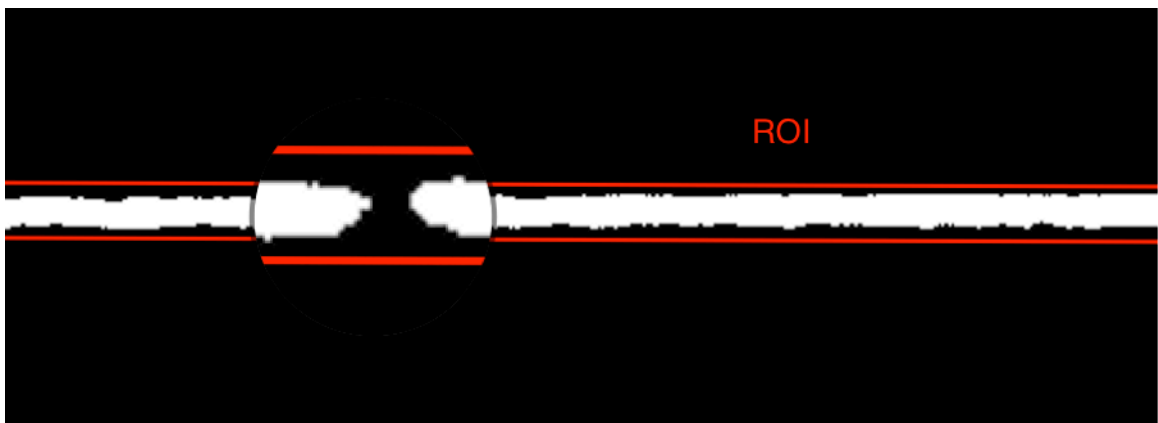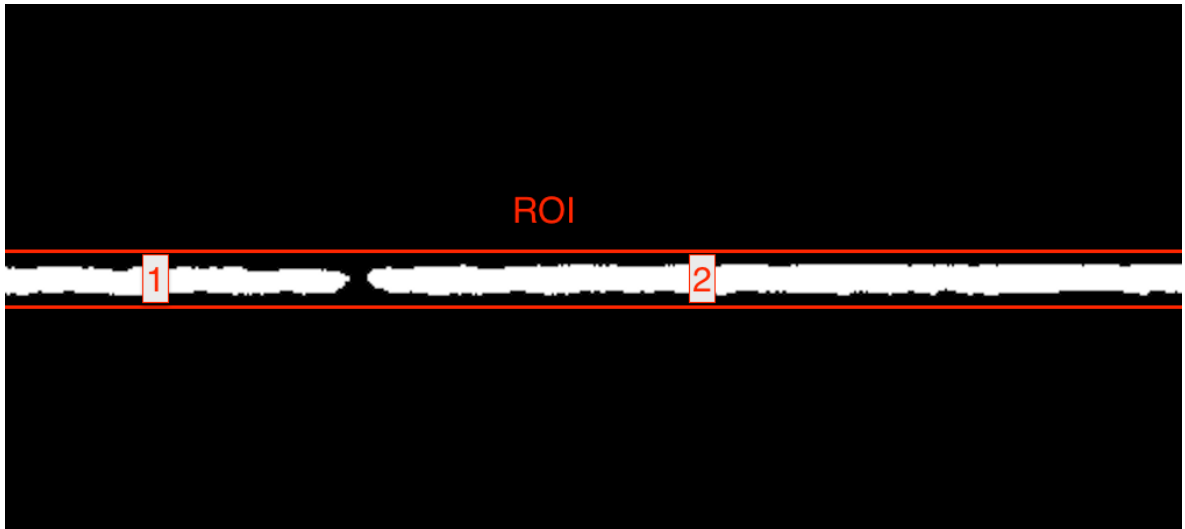**Figure 24.** Image ready for particle analysis (1. Particle number 1, 2. Particle number 2).

Performance of the defect detection can be defined by imaging surface where is an example one particle. By increasing triggering frequency step-by-step, analysis algorithms analyses more images during a second. After all CPU power is used, and maximum analysis speed is achieved, acquired images starting to fill the buffer of the FIFOs. The phenomena can be noticed from the user interface. Maximum analysis speed of laser scribing can be calculated multiplying maximum defect detection speed (fps) with the length of scribing line fitted in one frame. The camera parameters used for all experiments are presented in table 5.

Table 5. Camera parameters used in experiments.

Resolution (size of the ROI, height x width)	960 x 20 Pixel
Pixel Bit Depth	8 bit
Camera Link Clock	82 MHz
Tap geometry	10 tap
Camera Link mode	Full

7.3 Evaluation of defect detection algorithms reliability

Evaluation of reliability of the defect detection algorithms can be performed by analyzing images from a scribing line. Three 20 mm long lines are scribed to the 1 mm thick aluminum piece, which has 15 μm thick anodized coating. The laser parameters used in scribing are presented in table 6.

Table 6 Laser parameters used in experiments.

Laser parameters	Values
Power	20 W
Speed	2000 mm/s
Frequency	105 kHz
Pulse length	20 ns
Spot Size (diameter)	55 μm

The programmed scribing path is shown in figure 25. As it can be seen from the figure, one line is programmed without discontinuity, another with one 0.1mm long discontinuity and third with two 0.1mm long discontinuities. The programmed discontinuities on the lines are presenting defects in cribbing. The scribed lines on the coated aluminum are show in figure 26. The real length of the discontinuities is little less than programmed, the measured length being 80 μm.
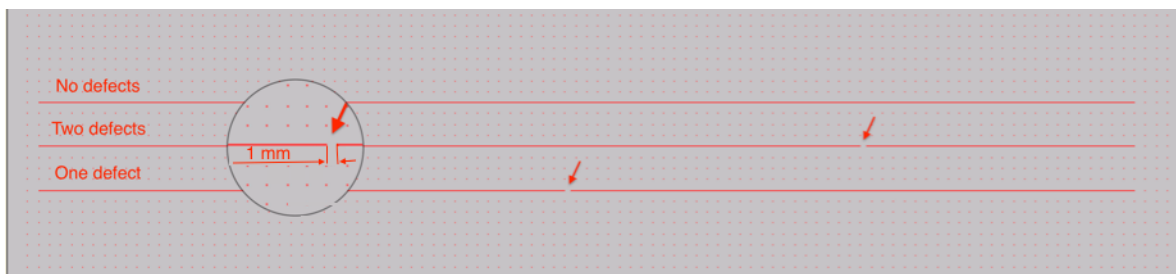

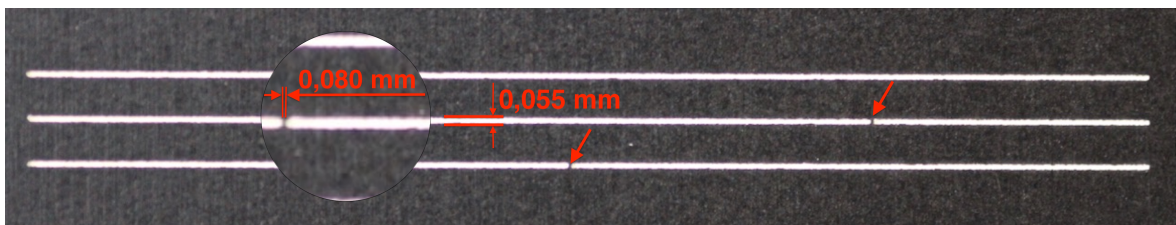**Figure 25.** CAD drawings in SAMLight laser control software.

Figure 26. Scribed lines for reliability experiments.

After the scribing process, the laser scanner is programmed to follow the same scribing path and the camera is set to imaging scribing line through the scan head. After imaging

and analyzing the whole path, a number of defects detected during the analysis should be same than a number of defects programmed to the path. Because the laser is turned off during the experiment, active laser illumination is not needed and it was replaced with four white LED lights for easier directing of the lightning. The LED lights were directed to the surface of the test piece from all directions (left, right, front and back) and as straight from up as it was possible when the smallest possible angle being about 25 degrees. The distance of the LED lights from the surface was about 9 cm. Required frame rate for the defect analysis can be calculated by dividing the laser processing speed by length of the scribing line in the ROI. In this case, the processing speed is set to 2000 mm/s and length of the measured scribing line is 4,7 mm. According to these values, needed frame rate for the analysis is 426 fps. For achieving small overlap in imaging, the speed is set to 430 fps.

7.4 Laser process monitoring experiment

Laser monitoring experiment are performed using same scribing path than in the previous experiment where reliability of defect detection algorithms were tested. The difference is that now the experiment is performed during the laser scribing process. Active laser illumination is used for lightning and the filter is set to the camera adaptor in front of the camera for filtering out all other light except lighting from the illumination laser, including reflected light from the pulsed laser. Illumination laser is directed as straight to perpendicular to the surface as it is possible, when the angle being about 45 degree. Physical dimensions of the illumination laser lens and the scan head set the limit for the angel.

8   EXPERIMENTAL RESULTS

8.1   Results of image acquisition and defect analysis performance experiment

As it can be seen in table 7, the maximum frame rate of the camera with resolution 960x20 is 10 900 fps. After that, the speed did not increase even if the camera was triggered faster. During the experiment, the FIFOs on the RT was not able to read the data as quickly than the data was written into the FIFOs on the FPGA causing data overflows in the RT's FIFOs. Maximum image acquisition speed without data overflows was 2 700 fps when the analysis algorithms and the displays were disconnected. Maximum defect detection speed was tested with the defect analysis algorithm using 1 500 μs exposure time and non-moving image. Image used for the experiment is shown in figure 27. As a result, the limit for the analysis speed was 560 fps. When the speed exceeded that limit, the buffers of the FIFOs on RT started to fill and analysis was not performed in real time anymore.

Figure 27. Image from the scribing line for the defect analysis performance experiment.

Table 7 Results of the image acquisition and defect analysis performance experiments.

Maximum camera frame rate	10 900 fps
Maximum Image acquisition speed from FPGA to RT	2 700 fps
Maximum defect analysis speed	560 fps

8.2   Results of defect detection algorithms reliability experiment

The reliability experiment was performed executing defect analysis for tree different scribing line. Camera frame rate was set to 430 fps, allowing one percent overlap in imaging and exposure time was set to 70 μs. Threshold range [10,255] provided best results and it is used in the experiment. The results are presented in table 8.

Table 8. Results of the defect detection algorithm reliability experiment.

Number of defects in scribing	0	1	2
Algorithm reliability experiment (Successful result / number of experiments)	10/10	10/10	10/10
Scribing monitoring experiment (Successful result / number of experiments)	NaN/10	NaN/10	NaN/10

In the scribing monitoring experiment, the defect analysis did work due difficulties with the illumination provided by active laser illumination. Images captured from the scribing line with the laser illumination are shown below. The image before image processing is shown in figure 28 and the threshold image is shown in figure 29.

Figure 28. Image from the scribing line captured with active laser illumination.
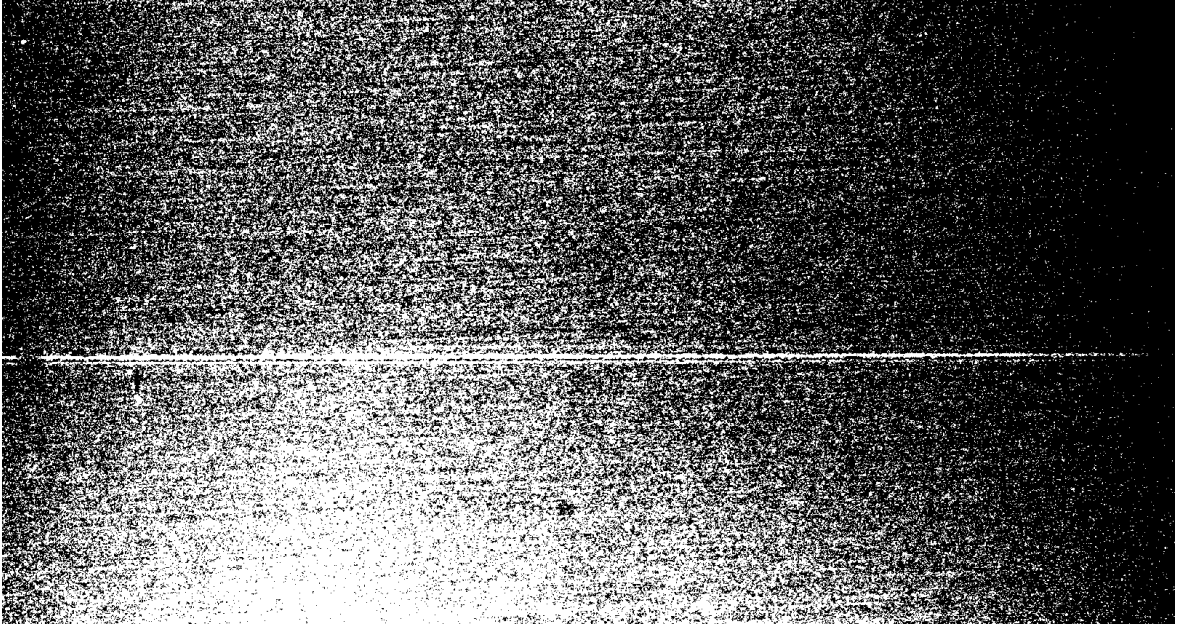
Figure 29. Threshold image from scribing line captured with active laser illumination.

9 ANALYSIS AND DISCUSSION

As it can be seen from the result, the maximum frame rate of the camera is 10900 fps, maximum image acquiring speed from the camera to FPGA and from FPGA to RT is 2700 fps and the maximum defect analysis speed is 560 fps. Image analysis speed can also be higher depending image under analysis. However, we can safely say that using 560 fps, the analysis is performed in real time. After 560 fps, the algorithm sometimes uses FOFOs memory as a buffer and analysis latency start to increase. It can be noticed from the results that the camera speed and image acquiring speed do not set the limit for the defect detection, but the limiting factor is defect analysis algorithm. If defect detection speed is needed to be increased, actions should be concentrated to improve the efficiency of analysis algorithms or increasing CPU power for faster analysis.

The reliability experiment of the defect detection algorithm was successful. The algorithm analyzed the scribing line 2 000 mm/s with 430 fps image analysis speed without any mistakes. Due fast movement of the scanned surface, it is necessary to use small exposure time for capturing sharp images from the scribing line. Therefore, the illumination was in the critical role. The illumination was implemented using white light from several directions directed straight to the test piece. If the analysis is needed to be performed faster, the exposure time should be decreased, and the power of illumination should be increased, that camera is able to gather enough light during the shorter exposure time. However, the power of the illumination is not only critical factor but also the direction of the lighting and many other variables influence the quality of the illumination. As it can be seen from the results of the laser process monitoring experiment with an active laser illumination, the experiment was not successful. The direction of the lighting was a problem because the laser illumination was demanding to be directed properly due that the lens of illumination laser was beside of scan heads lens. The lens was impossible to be directed perpendicular to the test piece. Therefore, most of the light was reflected away from the camera and only small amount of light was gathered to the cameras sensor. Because of powerful laser illumination, the camera was able to collect enough light, but a lot of light was also reflected from surrounding surface to the sensor causing poor contrast between the scribing line and the surrounding surface. Without good contrast, performing

reliable defect analysis is impossible. For the better results, the illumination should be replaced.

Used laser in experiments was a nanosecond pulsed laser. According to the study performed in theoretical part of this paper, marking quality of a picosecond laser is sharper than nanosecond laser. Image analysis is always easier to implement if details in the image are sharp. We can assume that the defect detection algorithms also work with the faster lasers. However, the monitoring system used in experiments is designed to work with this particular laser setup. If monitoring is implemented in different laser process applications, it is possible that example the camera adapter should be designed to meet requirements of the particular laser system. In addition, problems with directing of active laser illumination should be solved.

10 CONCLUSIONS AND SUMMARY

The purpose of the study was finding a method for monitoring of laser scribing process with a high-speed camera in real time and evaluating performance and reliability of the method. The study was divided into a theoretical and an experimental part.

In the theoretical part, first, some study was carried out to get knowledge from a digital camera and machine vision technology. The knowledge was used for choosing the proper camera and for setting the camera parameters for fast imaging. In addition, some study was carried out for helping in development of image processing and analysis algorithms. It was also important to improve knowledge in laser scribing technology and study existed laser-monitoring applications. It was concluded that existed monitoring systems are typically implemented to monitor laser processes such a laser welding, where the speed of the process is sufficient low. The speed of the existed monitoring applications is not fast enough to implement real-time monitoring in laser scribing applications. That means the new monitoring system was needed to be developed which can detect defects during the fast laser processes. According to the study in theoretical part, there could be market potential for fast real time laser scribing process monitoring application, an example in solar cell technology, where benefits of the laser scribing are studied.

In the experimental part of the study, the test setup was developed for fast real-time monitoring. Chosen high-speed camera for the imaging was Basler acA2000-340km, which is Camera Link camera with CMOS sensor. The camera provides ten taps parallel pixel readout from the sensor and flexible ROI selection. High performance PXI-system was built to execute image processing and defect analysis. The choice of image analysis algorithm for the defect analysis is based on particle analysis due its simplicity. Simple algorithm can analyze images faster than complicated algorithm such pattern recognition.

Purpose of the experiments is evaluating performance and reliability of the monitoring system. Preferring to the results, the maximum defect detection speed is 560 fps, when the defect analysis sets the limit for the maximum speed. The reliability of the defect detection

was evaluated with two experiments. The first experiment was performed imaging the scribing line when the laser was turned off. The laser scanner was programmed to follow in advance scribed line 2000 mm/s, while the defect detection was set to execute analysis 430 fps. Illumination was implemented using white light source from multiple directions. The experiment was successful, and defect analysis algorithm did not miss any defects during the experiment. The second experiment was performed during the laser process. The experiment was similar than the first one, but now laser was turned on. The purpose was to monitor the process and find the defects during the laser process. The results were not as good as in first experiment without laser. Because laser was on, the white light illumination had to be replaced with powerful active laser illumination. However, directing of the laser illumination was demanding and it was hard to get enough contrast between scribing line and surrounding surface. Performing defect analysis was impossible due poor illumination. However, according to the results of experiments it can be concluded that error detection algorithms work with proper illumination and method for real-time laser scribing monitoring is found.

REFERENCES

Alper, G. 2011. CCD vs. CMOS sensors in machine vision cameras [Online document]. [Accessed 11 February 2016]. Available: http://info.adimec.com/blogposts/bid/39656/ CCD-vs-CMOS-Image-Sensors-in-Machine-Vision-Cameras

Bailey, D, 2012. Implementing Machine Vision Systems Using FPGAs. London: Springer, p. 34

Basler. acA2000-340km. [Online document]. [Accessed 16 March 2016]. Available: http://www.baslerweb.com/en/products/cameras/area-scan-cameras/ace/aca2000-340km

Batchelor, B. G. 2012 Algorithms, Approximations and Heuristics. London: Springer. 78 p.

Burn, A., Heger, C., Buecheler, S., Nishiwaki, S., Tiwari, A., Ziltener, R., Bremaud, D., Krainer, L., Spuehler, G. & Romano, V. 2015. All laser scribing for monolithic interconnection of Cu(In,Ga)Se thin film solar cells Optimization, validation, and assessment for industrial production [Online document]. [Accessed 16 March 2016]. Available: http://www.swissolar.ch/fileadmin/user_upload/Tagungen/PV-Tagung_2015/ Posterausstellung/P1_Burn_BFH-ALPS__PV-Tagung_Basel_2015.pdf

Chen, H., Lv, F., Lin, T. & Chen, S. 2009. Closed-Loop Control of Robotic Arc Welding System with Full-penetration Monitoring, vol. 56. pp. 565–578.

Eberhardt, G., Banse, H., Wagner, U. & Peschel, T. 2010. Structuring of thin film solar cells, Proc.

Fennander, H., Kyrki, V., Fellman, A., Salminen, A. & Kälviäinen, H. 2009. Visual measurement and tracking in laser hybrid welding. Machine Vision and Applications, Vol. 20, Iss. 2. pp. 103–118.

Fidali, M. & Jamrozik, W. 2013. Diagnostic method of welding process based on fused infrared and vision images. Infrared Physics & Technology, Vol. 61. pp. 241–253.

Fintel, R. 2013. Comparison of the Most Common Digital Interface Technologies in Vision Technology [Online document]. [Accessed 11 February 2016]. Available: http://s.baslerweb.com/media/documents/BAS1302_White_Paper_Interface_Comparsion_ EN.pdf

Gilblom, D. L. 2012. Cameras. London: Springer. 122 p.

Huang, W. & Kovacevic, R. 2012. Development of a real-time laser-based machine vision system to monitor and control welding processes. The International Journal of Advanced Manufacturing Technology, Vol. 63, Iss. 1. pp 235–248.

Liu, Z., Ukida, H., Niel, K. & Ramuhalli, P. 2015. Industrial Inspection with Open Eyes: Advance with Machine Vision Technology. Integrated Imaging and Vision Techniques for Industrial Inspection. Part of the series Advances in Computer Vision and Pattern Recognition. pp. 1–37.

Lucas, L. & Zhang, J. 2012. Femtosecond laser micromachining: A back-to-basics primer [Online document]. [Accessed 16 March 2016]. Available: http://www.industrial-lasers.com/articles/2012/06/femtosecond-laser-micromachining-a-back-to-basics-primer.html

National Instruments. 2010a. Thresholding [Online document]. [Accessed 16 March 2016]. Available: http://zone.ni.com/reference/en-XX/help/372916J-01/nivisionconcepts/ thresholding/

National Instruments. 2010b. Edge Detection [Online document]. [Accessed 16 March 2016]. Available: http://zone.ni.com/reference/en-XX/help/372916J-01/nivisionconcepts/ edge_detection_concepts/

National Instruments. 2010c. Pattern matching [Online document]. [Accessed 16 March 2016]. Available: http://zone.ni.com/reference/en-XX/help/372916J-01/nivisionconcepts/pattern_matching_whento/

National Instruments. 2010d. Particle analysis [Online document]. [Accessed 16 March 2016], Available: http://zone.ni.com/reference/en-XX/help/372916J-01/nivisionconcepts/particle_analysis/

Purtonen, T., Kalliosaari, A. & Salminen, A. 2014. Monitoring and Adaptive Control of Laser Processes. Physics Procedia; 8th International Conference on Laser Assisted Net Shape Engineering LANE 2014, Vol. 56. pp. 1218–1231.

Rekow, M., Murison, R., Panarello, T., Dunsky, C., Dinkel, C., Nikumb, S., Pern, J. & Mansfield, L. 2010. CIGS P1, P2, P3 Scribing Processes using a Pulse Programmable Industrial Fiber Laser.

Rofin. Laser Scribing Eases the Further Mechanical Processing [Online document]. [Accessed 16 March 2016]. Available: https://www.rofin.com/en/applications/laser-structuring/laser-scribing/

SCANLAB. 2015. Camera Adapter. [Online document]. [Accessed 16 March 2016]. Available: http://www.scanlab.de/sites/default/files/PDF-Dateien/Data-Sheets/Camera%20adapter_EN_0.pdf

Steen, M.W. & Mazumder, J. 2010. [Chapter 1] Background to Laser Design and General Applications. In: Steen, M.W. & Mazumder, J. Laser Material Processing. 4th edition. Springer. pp. 11–78.

Teledyne Dalsa. Application notes and technology primer: CCD versus CMOS [Online document]. [Accessed 11 February 2016]. Available: https://www.teledynedalsa.com/imaging/knowledge-center/appnotes/ccd-vs-cmos/
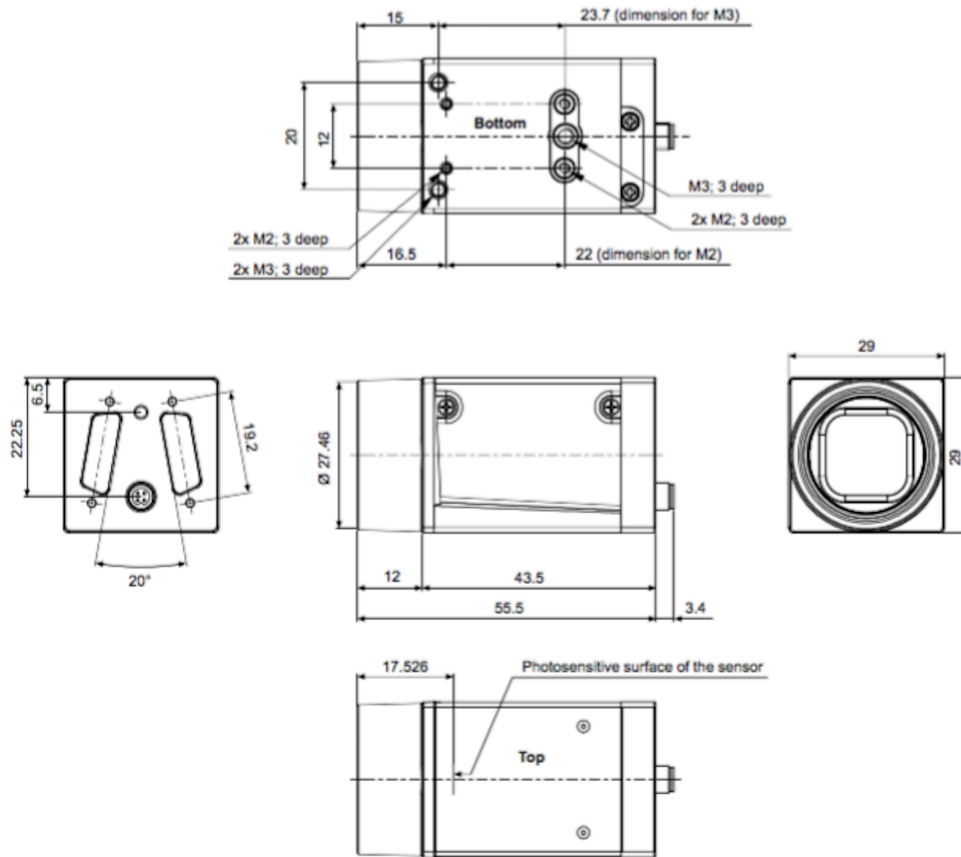
Tenner, F., Brock, C., Klämpfl, F. & Schmidt, M. 2015. Analysis of the correlation between plasma plume and keyhole behavior in laser metal welding for the modeling of the keyhole geometry. Optics and Lasers in Engineering, Vol. 64. pp. 32–41.

TECHNICAL MEASUREMENTS.
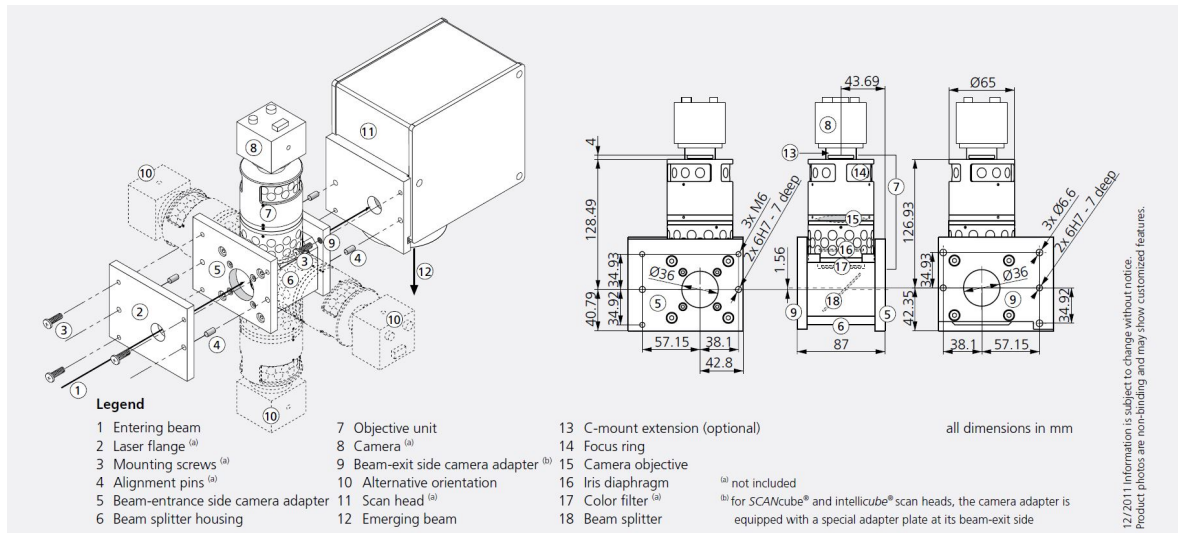
Installation drawings of the monitoring adapter into the scan head (SCANLAB, 2015, p 2).

Mechanical dimensions of Basler asA2000-340km high-speed camera (Basler, 2015, p. 8).